

# DARTS: DEFORMABLE ANIMATION READY TEMPLATES FOR CLOTHING HUMANS

Shashikant Verma, Shanmuganathan Raman\*

Indian Institute of Technology Gandhinagar, India  
`{shashikant.verma, shanmuga}@iitgn.ac.in`

## ABSTRACT

Accurate 3D modeling of humans and high-fidelity garments is crucial in computer vision and graphics, impacting gaming, virtual, and augmented reality applications. While recent data-driven approaches have progressed in estimating segregated geometries for clothed humans, they often struggle with the seamless integration required for physics-based simulations. We introduce Deformable Animation Ready Templates (DARTs) to address these challenges, which enhance template-based garment reconstruction. Our framework employs a robust feature-line regressor network to establish precise deformation constraints guided by input image characteristics. Additionally, we present a novel differentiable Constrained Rigid Deformation Layer (CRDL) that facilitates effective template deformation while preserving the essential geometry of the garment. Our experiments demonstrate that DARTs can generate templates for physics-based simulation, allowing for seamless garment animations influenced by dynamic environmental factors. With minor adjustments, our templates can accommodate various clothing categories, promoting diversity in animated garment modeling.

**Index Terms**— 3D Garment Reconstruction, Template-based Clothing, Deep Learning.

## 1. INTRODUCTION

The 3D modeling of humans and high-fidelity wearable garments is pivotal in computer vision and graphics. These geometric representations enable photorealistic and essential applications in virtual live-streaming, gaming, filming, visual effects, and virtual/augmented reality. Initially, methods employed reconstruction techniques using a single surface (mesh or voxel) to represent both clothing and the body. Consequently, such approaches could not separate the clothing from the subject in the image, which restricted their applicability in garment-specific applications and significantly hindered

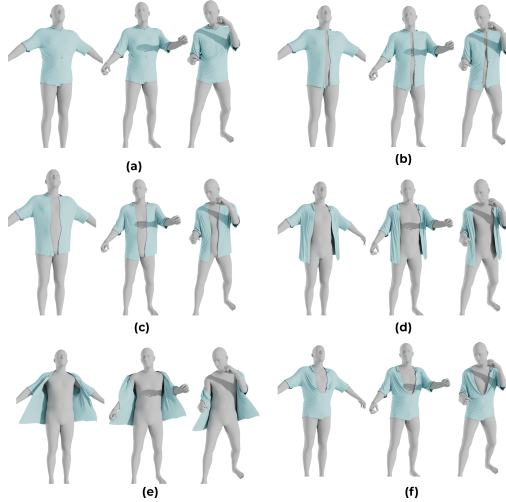


**Fig. 1:** The effects of manipulating spring constraints defined on the proposed DART templates. In (a), the spring ends are merged (welded), (b) high spring strength, followed by progressively loosening in (c) and (d). (e) shows repulsive spring forces, and (f) showcases the effect of partially applying spring forces along the seams, facilitating garment openings.

realistic animation capabilities. The rise of deep learning techniques for recovering unclothed human shapes and poses from multiple or even single images [1, 2] has yielded remarkable results. Recent advancements focus on enhancing realism and providing greater control over garment reconstruction by learning the geometries of humans and wearables separately. To capture complex geometry beyond just human body shape, several non-parametric, voxel-based, and implicit representations have been introduced [2–5].

To faithfully reconstruct an animation-ready garment template that captures the clothing characteristics from a single image, we propose **Deformable Animation Ready Templates** (DARTs) for clothing humans. In this work, we propose a robust feature-line regressor network, which is essential for setting accurate constraints for deformation. We utilize templates derived from the SMPL model of humans [6], and enhance them with function-

\* This work is supported by Jibaben Patel Chair in AI.

alities essential to garment draping. We refer to our modified templates as DARTs. Our central insight is that the deformation of templates must also be guided by the characteristics of the input image, known human shape priors, and the regressed feature lines. To achieve this, we propose a novel differentiable Constrained Rigid Deformation Layer (CRDL) to deform the templates effectively. Through experimental validation, we show that our deformed templates are ready for physics-based simulation, influenced by the factors set during deformation by the CRDL layer, thereby fully automating the process. With minimal adjustments, our templates can also be adapted to generate a variety of clothing.

**Contributions.** In summary, our contributions are three-fold. **1.** We propose a Spatial-Transformer-based, image-guided Graph Neural Network (GNN) for feature line regression specifically designed to estimate feature lines accurately. **2.** We introduce a novel differentiable Constrained Rigid Deformation Layer (CRDL) for deforming garment templates, constraining deformation on diverse factors. This approach for deformation achieves superior results compared to traditional techniques and enables physics-based simulation-ready templates that can adapt to various clothing categories. **3.** We enhance templates derived from SMPL human body priors by equipping them with simulation-ready capabilities and refer to them as Deformable Animation Ready Templates. We demonstrate the clothing simulations generated on AMASS sequences using DARTs.

## 2. RELATED WORK

Garment reconstruction approaches can be broadly classified into template-free and template-based methods. This section reviews prior studies relevant to our work.

**Garment Reconstruction With Templates.** Starting with human shape as prior [7] model garments as offsets from human body shape and learn a displacement vector for each body vertex to construct skin-tight garments. BCNet [8] initially generates a basic template mesh using PCA and then enhances surface details through an image-guided graph attention network. MultiGarment-Net (MGN) [9] predicts category-specific garments and body shapes by training a deep learning model on large-scale digital wardrobe. SMPLicit [10] introduces a topology-aware generative model to represent garment geometry. Building on templates derived from the SMPL human model [6], methods like [11,12] propose an explicit template fitting on implicit representations to regress clothed geometry. These methods primarily focus on estimating static meshes by capturing fine surface details, which are often less relevant for garment animation, as the estimated deformations are ultimately overridden by factors like gravity, wind, collision, and ma-

terial properties during physics-based simulation. These physical factors dynamically influence the garment’s behavior in real-time, adjusting its drape, folds, and wrinkles in response to the surrounding environment and motion, making initial surface detail less impactful.

**Animation Ready Clothing Templates.** Classical mass-spring and position-based modeling methods [13] enhance simulation efficiency, though with trade-offs in speed. These advancements enable methods such as [14] to model garments as panel-based structures with predefined sewing patterns, creating diverse datasets through simulation. NeuralTailor [15] infer sewing patterns and panels from 3D point clouds. PanelFormer [16] utilizes a transformer-based network to estimate panels and stitches given a single image. Similarly, [17] uses SMPL templates for draping various garment styles; however, this method is limited to close-fitting garments like shirts and pants and does not effectively model looser or more complex garments, such as long dresses and skirts. More recently, [18] explored reconstructing real-world garments employing Gaussian splitting [19].

## 3. METHODOLOGY

Given a single image  $\mathcal{I}$ , we aim to generate simulation-ready garment geometry that integrates smoothly with physics-based simulation (PBS) frameworks. Our approach begins by building garment templates on the SMPL human body model, represented as the parametric function  $M(\cdot)$ , which depends on both pose ( $\theta \in \mathbb{R}^{3 \times 24}$ ) and shape ( $\beta \in \mathbb{R}^{10}$ ) parameters [6]. Our garment templates are built on top of  $M(\cdot)$ , aligning with previous approaches [11, 12, 20]. Initially, we adjust the per-vertex segmentations in the standard SMPL model [6] to suit our needs better, mainly refining areas such as the shoulders and hemline, as shown in Figure 2(a). Our garment templates cover 12 common clothing categories from the DeepFashion-3D Dataset [11], including long/short/no-sleeve tops, long/short/no-sleeve dresses, as well as long/short pants and skirts. We utilize pose and shape parameters provided in the dataset directly, and, in the case of inference on real images, an off-the-shelf parameter regressor like PyMAF [21] could be employed. To form templates for specific garment categories, we combine only the relevant segments, excluding geometry related to the head, palms, and feet in all template categories, as these areas are irrelevant to garment geometry. All segment boundaries are used to form a collection of initial feature lines, denoted as  $F_{smpl}$  (Figure 2(b)). In contrast, the feature lines for a specific garment template  $T_g$  are represented as  $F_g \subset F_{smpl}$ . For example, for the no-sleeve dress category, the extracted garment template  $T_g$  is shown in Figure 2(c), and the initial garment feature lines  $F_g$  are highlighted in green

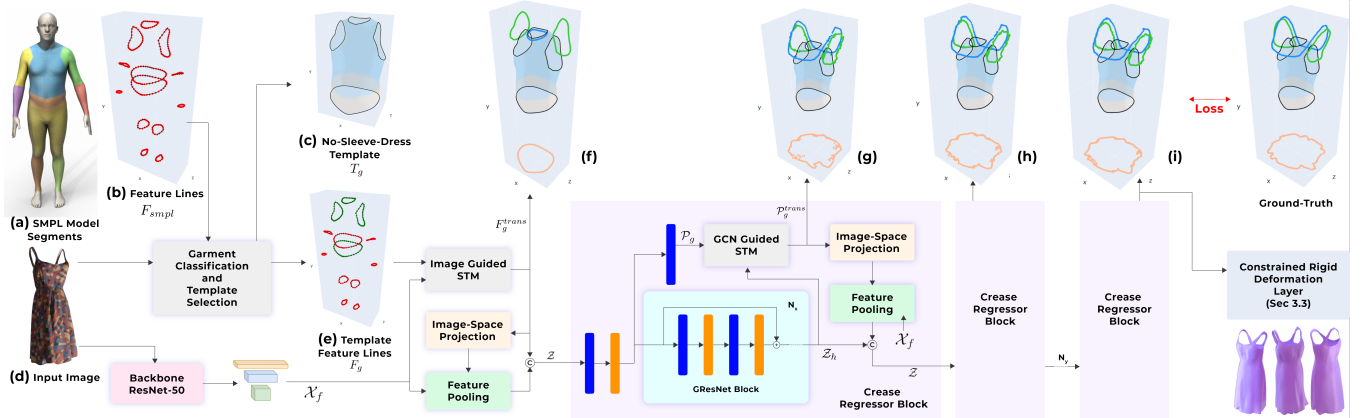


**Fig. 2:** Given an input image, denoted as  $\mathcal{I}$  (d), we begin by selecting a template  $T_g$  (c) and the corresponding feature lines  $F_g$  (e) derived from the posed SMPL human model  $\mathcal{M}$  (a). The complete set of possible feature lines across all garments, denoted as  $F_{smpl}$ , is shown in (b). We then apply image-guided spatial translations to  $F_g$ , utilizing features  $X_f$  extracted from ResNet-50 to obtain the translated feature lines  $F_g^{trans}$ . Finally, we refine this output through multiple CRB blocks to produce the regressed feature lines,  $P_g^{trans}$ . The intermediate outputs after the Image-Guided STM module and the GCN-guided STM modules are shown in (f), (g), (h), and (i). Legend: ■ Graph Convolution Layer, and □ ReLU activation.

in Figure 2(e). Every  $i$ -th feature line  $f_i$  forms an edge loop, with each vertex having precisely two neighbors.

**Feature Line Regression Network** Given our focus on robustly estimating accurate feature lines, we extend the baseline approach of [11, 22] and introduce a Spatial-Transformer-based, image-guided feature line regression network. The feature line regression network, as shown in Figure 2, takes as input the image  $\mathcal{I}$ , feature lines  $F_{smpl}$  and camera  $\mathcal{C}$  as input and predicts the final 3D-feature lines reflecting boundary details from the input image. In terms of architecture, our Regression Network differs from [11] with the key difference that it employs an Image-Guided and GCN-Guided Spatial Transformer Module. To select the appropriate garment template  $T_g$  and feature lines  $f_g$  from  $F_{smpl}$ , we finetune a ResNet-50 architecture for classification on the Deep-Fashion3d Dataset. On our synthetic dataset, we use 90% for training and achieve a classification accuracy of 99.4% on the validation set. Utilizing camera parameters  $\mathcal{C}$ , calculated w.r.t. T-posed SMPL, we project the translated points onto the spatial resolution of  $i$ -th feature map  $X_i \in \mathcal{X}_f$  and pool the features for all  $i$ , similar to [22]. This process is represented by the *Image-Space Projection* and *Feature Pooling* blocks in Figure 2. Afterward, we concatenate pooled features with vertex locations, resulting in  $\mathcal{Z}$ , where each vertex in  $f_i$  has its corresponding pooled feature of  $q$ -dimensionality, such that  $z_i \in \mathbb{R}^{n_i \times (q+3)}$ . These concatenated features are passed through multiple *Crease Regressor Blocks* to produce the final feature lines. Based on the garment category in the input image, STM Modules predict a spatial translation vector for each feature line  $f_i \in \mathbb{R}^{n_i \times 3}$  within  $F_g$ . Image-Guided Spatial Transformer takes  $X_f$

as input and outputs a global translation vector for each feature line  $f_i$  in Template  $T_g$ . In contrast, GCN-Guided STM takes high-dimensional per-vertex features  $P_g$  and outputs per-vertex translations to facilitate fine movements of vertices for crease-line fitting. The feature lines after global and per-vertex translations are shown in Figure 2(f) and Figure 2(g-i), respectively. The addition of STM Modules improves the regression capability of the network, as we discuss in Section 4. Similar to [11], we utilize Chamfer loss  $L_c$  with edge regularization  $L_{ed}$  to supervise the network during training. However, this loss alone does not ensure that the feature lines form a single continuous circular loop, which is essential for the robust deformation of the template. We train the network with additional circularity loss  $L_{circ}$  to address this. A detailed explanation of spatial transformers and the loss functions is provided in the supplementary material.

$$L_{ce} = \sum_{i=0}^{N_y+1} L_c(F_g, X_g^i) + \lambda_1 \sum_{i=0}^{N_y+1} L_{ed}(X_g^i) + \lambda_2 L_{circ}^i \quad (1)$$

**Constrained Rigid Deformation Layer.** We employ detail-preserving deformations by applying the as-rigid-as-possible (ARAP) technique, as proposed by [25], which minimizes deviations from rigidity by penalizing changes in local vertex neighborhoods. In contrast to [25], which minimizes the ARAP energy through an iterative least-squares approach, we introduce a differentiable computation of the ARAP energy using the CRDL Layer. Specifically, we design the CRDL layer for the template  $T_g$ , with its vertices  $v_T \in \mathbb{R}^{V \times 3}$ , treated as learnable parameters. To determine the optimal parameters  $v_T$ , we minimize (a) the ARAP energy and (b) the

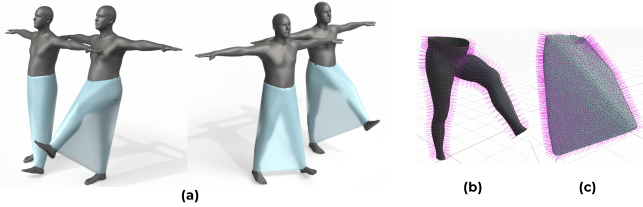


**Fig. 3:** Fitting to a given shape prior is challenging for garments in dress categories, such as skirts, that cover both legs. We estimate the hull mesh (c) for the lower body (a) and guide the garment vertices to move along the outward normals of the hull mesh (c) rather than those of (b). The normal directions are indicated by pink arrows (Zooming in is recommended).

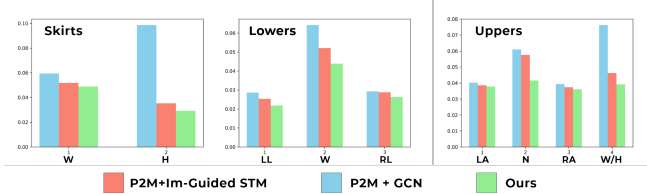


**Fig. 4:** A quantitative crease-wise comparison of chamfer distance across different garment groups with **P2M + GCN** [11]. **P2M + Im-Guided STM** highlights the impact of incorporating the proposed crease-wise global translations. Significant improvements are observed, especially in feature lines **N** and **H** that undergo large transformations. Crease Labels: W (Waist), LL (Left Leg), RL (Right Leg), LA (Left Arm), RA (Right Arm), N (Neckline), H (Hemline).

fitting constraint losses in an iterative process using the ADAM optimizer. This optimization is performed based on the final positions of the vertices defining the crease feature lines  $P_g^{trans}$  predicted by the Feature Line Regressor.

**(a) ARAP Energy.** The ARAP energy quantifies the deviation from rigidity by penalizing the alterations in local vertex neighborhoods between the original and deformed meshes. Mathematically, the ARAP energy  $\mathcal{E}$  for a deformation is defined as described in Equation 2.

$$\mathcal{E} = \sum_i \sum_{j \in \mathcal{N}(i)} w_{ij} \|(p'_i - p'_j) - R_i(p_i - p_j)\|^2 \quad (2)$$

Here,  $i$  represents the index of a vertex in  $v_i \in v_T$ , with its neighborhood defined as  $\mathcal{N}(i)$ . The vertex locations  $p_i$  and  $p_j$  refer to positions in the template mesh  $T_g$ , while  $p'_i$  and  $p'_j$  denote positions in the deformed mesh. Unlike the hard constraints set for  $v_i \in F_g$  to move to  $P_g^{trans}$  as in [25], our  $p'_i$  and  $p'_j$  are learnable parameters from the CRDL layer, which will be optimized by minimizing the energy defined in Equation 2.  $w_{ij}$  is the per-edge cotangent weight, and  $R_i$  is a local rotation matrix for vertex  $v_i$ , capturing the optimal rigid rotation for that vertex's neighborhood. For a detailed explanation of the

Method	P2M-GCN [11]			Im-Guided STM			Ours		
	Upper	Lower	Skirts	Upper	Lower	Skirts	Upper	Lower	Skirts
CD	0.217	0.122	0.158	0.18	0.106	0.087	0.155	0.092	0.078

**Table 1:** Chamfer distance between the predicted and ground truth feature lines.

method, we refer readers to [25], with additional context provided in the supplementary material.

**(b) Fitting Constraints.** Deforming  $T_g$  solely through the handle constraints on feature lines, as described by [25], often leads to mesh penetration into the human body  $M(\beta, \theta)$ , which is undesirable for clothing simulations. For each vertex  $v_i \in T_g$ , we first identify the nearest vertex  $v_i^{near} \in M$  and calculate the signed distance  $s_i$ , which considers the direction relative to the normal  $n_i^{near}$  at the nearest vertex. Specifically,  $s_i = d_i$  if  $(v_i - v_i^{near}) \cdot n_i^{near} > 0$ , and  $s_i = -d_i$  otherwise. To prevent penetration, we encourage each vertex  $v_i$  with  $s_i < 0$  (i.e., inside the target surface) to move in the direction of the outward normal. We impose the following loss, defined in Equation 3, where  $\mathcal{V}_{in}$  is the set of all vertices with  $s_i < 0$ .

$$L_{fit} = \frac{1}{|\mathcal{V}_{in}|} \sum_{i \in \mathcal{V}_{in}} (v_i - v_i^{near}) \cdot n_i^{near} \quad (3)$$

As per Equation 3, fitting to the SMPL body prior ( $M$ ) presents a challenge for garments in dress categories, like skirts, that span both legs. To address this, we estimate the convex hull of the lower body, re-mesh it isotropically, and apply the fitting loss on this modified body model, where the lower part is replaced by the estimated hull mesh instead of using  $M$  directly. This is illustrated in Figure 3. Since the deformation resulting from minimizing Equation 2 only aligns the outermost feature lines, we also apply a silhouette loss  $L_{sil}$  based on the segmented garment in the input image  $\mathcal{I}$  and the rendering of the template  $T_g$  from the viewpoint of the camera  $\mathcal{C}$ .

**Animation Ready Templates.** We create commonly used seams as outlined by [14, 15], enabling templates to be reorganized into multiple panels, as shown in Figure 7(a,b). We then add spring-based constraints between the separated panels. The created seams could also be extended to stitch accessories, such as ties and collars, as illustrated in Figure 7(c). Figure 1 highlights how manipulating spring constraints enables diverse simulation capabilities. Additionally, in Figure 5, we present clothing simulations performed on a template obtained after CRDL deformation.

## 4. RESULTS

Our network is trained using a synthetic dataset derived from the registered scans and annotations provided by the DeepFashion3D Dataset [11]. This dataset consists



**Fig. 5:** Simulation results obtained within Maya software on an AMASS [23] sequence for a deformed template.

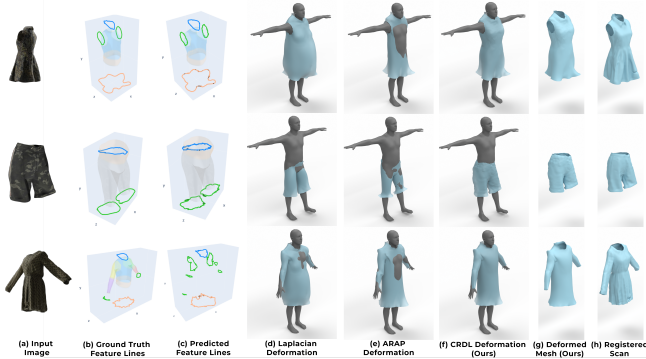


**Fig. 6:** Qualitative comparison of template deformations: handle-based mesh deformation [11, 24] (d), ARAP deformation [25] (e), and CRDL Layer-based deformation (f). Feature line regression results by our method (c) vs. ground truth (b) for the input image (a). Final deformed mesh via CRDL Layer (g) and corresponding registered garment scans (h) are shown. Zoom-in recommended.

of 1,212 registered garment scans across nine clothing categories. We set aside 10 garment scans for each category to conduct quantitative and qualitative analysis. In Table 1, we report the chamfer distance between predicted and ground truth feature lines, organized by garment category. Applying spatial translations to crease-wise features shows significant performance improvement over P2M-GCN [11], particularly on hemlines and necklines, as these creases tend to exhibit greater spatial transformations. In contrast to our approach, [12] effectively estimates feature lines from implicit representations. However, we cannot directly compare as the model is not publicly available. Additionally, their method is computationally intensive due to the learning of implicit representations. Figure 4 displays crease-wise Chamfer distances, emphasizing the substantial improvements achieved by our proposed approach, particularly in the bar plots labeled hemlines (H) and necklines (N). In Table 1 and Figure 4, Im-Guided STM represents the feature line network that includes only the Image-Guided STM, omitting the GCN-Guided STMs from the regression network, as depicted in Figure 2. Notably, further improvements are observed when fine translations are guided by GCN-Guided STMs in the Crease Regression blocks, demonstrated in the results labeled as Ours in

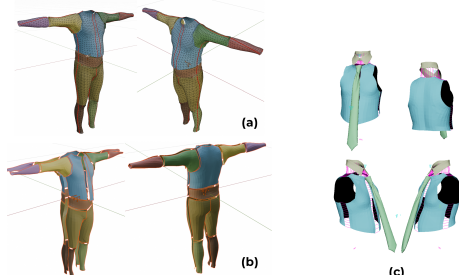


**Fig. 7:** Predefined seams (a) and the separation of components along these seams to generate DARTs (b). The resulting detached vertices are connected using spring constraints. (c) demonstrates the addition of external accessories to the predefined seams of the template, along with spring constraints in pink (Zooming in is recommended).

Table 1 and Figure 4. In Figure 6, we present the deformation of the template mesh  $T_g$  using the proposed CRDL-Layer, compared with [11, 24, 25] in the context of garments. The deformed mesh, with DARTs stitch constraints, can be directly imported into standard graphics software for draping simulations, as presented in Figure 5 and Figure 1.

**Supplementary Material.** The supplementary material, available at [Link](#), includes a detailed explanation of all network modules including spatial transformers, loss functions, synthetic data curation, depth ablation analysis, optimization parameters for the CRDL Layer, implementation details, and additional qualitative results.

## 5. CONCLUSION

We introduce Deformable Animation Ready Templates (DARTs) as an effective and practical solution for realistic garment reconstruction and animation within physics-based simulation frameworks. Our method incorporates a robust feature-line regression network and a novel Constrained Rigid Deformation Layer (CRDL). This design enables precise, image-guided deformations that incorporate human shape priors and capture intricate details of the garments. The proposed approach generates simulation-ready templates, significantly reducing the need for manual post-processing.

## 6. REFERENCES

- [1] Angjoo Kanazawa, Michael J Black, David W Jacobs, and Jitendra Malik, “End-to-end recovery of human shape and pose,” in *Proceedings of the IEEE conference on computer vision and pattern recognition*, 2018.
- [2] Gul Varol, Duygu Ceylan, Bryan Russell, Jimei Yang, Ersin Yumer, Ivan Laptev, and Cordelia Schmid, “Bodynet: Volumetric inference of 3d human body shapes,” in *Proceedings of the European conference on computer vision (ECCV)*, 2018, pp. 20–36.
- [3] Zerong Zheng, Tao Yu, Yixuan Wei, Qionghai Dai, and Yebin Liu, “Deephuman: 3d human reconstruction from a single image,” in *Proceedings of the IEEE/CVF International Conference on Computer Vision*, 2019.
- [4] Shunsuke Saito, Tomas Simon, Jason Saragih, and Hanbyul Joo, “Pifuhd: Multi-level pixel-aligned implicit function for high-resolution 3d human digitization,” in *Proceedings of the IEEE/CVF conference on computer vision and pattern recognition*, 2020, pp. 84–93.
- [5] Thiemo Alldieck, Gerard Pons-Moll, Christian Theobalt, and Marcus Magnor, “Tex2shape: Detailed full human body geometry from a single image,” in *Proceedings of the IEEE/CVF International Conference on Computer Vision*, 2019, pp. 2293–2303.
- [6] Matthew Loper, Naureen Mahmood, Javier Romero, Gerard Pons-Moll, and Michael J Black, “Smpl: A skinned multi-person linear model,” in *Seminal Graphics Papers: Pushing the Boundaries, Volume 2*, 2023.
- [7] Yuliang Xiu, Jinlong Yang, Dimitrios Tzionas, and Michael J Black, “Icon: Implicit clothed humans obtained from normals,” in *2022 IEEE/CVF Conference on Computer Vision and Pattern Recognition (CVPR)*. IEEE, 2022, pp. 13286–13296.
- [8] Boyi Jiang, Juyong Zhang, Yang Hong, Jinhao Luo, Liangang Liu, and Hujun Bao, “Bcnet: Learning body and cloth shape from a single image,” in *Computer Vision-ECCV 2020: 16th European Conference, UK, August 23–28, 2020, Proceedings, Part XX 16*. Springer, 2020.
- [9] Bharat Lal Bhatnagar, Garvita Tiwari, Christian Theobalt, and Gerard Pons-Moll, “Multi-garment net: Learning to dress 3d people from images,” in *Proceedings of the IEEE/CVF international conference on computer vision*, 2019, pp. 5420–5430.
- [10] Enric Corona, Albert Pumarola, Guillem Alenya, Gerard Pons-Moll, and Francesc Moreno-Noguer, “Smplicit: Topology-aware generative model for clothed people,” in *Proceedings of the IEEE/CVF conference on computer vision and pattern recognition*, 2021, pp. 11875–11885.
- [11] Heming Zhu, Yu Cao, Hang Jin, Weikai Chen, Dong Du, Zhangye Wang, Shuguang Cui, and Xiaoguang Han, “Deep fashion3d: A dataset and benchmark for 3d garment reconstruction from single images,” in *Computer Vision-ECCV 2020: 16th European Conference, UK, August 23–28*. Springer, 2020.
- [12] Heming Zhu, Lingteng Qiu, Yuda Qiu, and Xiaoguang Han, “Registering explicit to implicit: Towards high-fidelity garment mesh reconstruction from single images,” in *Proceedings of the IEEE/CVF Conference on Computer Vision and Pattern Recognition*, 2022.
- [13] Matthias Müller, Bruno Heidelberger, Marcus Hennix, and John Ratcliff, “Position based dynamics,” *Journal of Visual Communication and Image Representation*, vol. 18, no. 2, pp. 109–118, 2007.
- [14] Maria Korosteleva and Sung-Hee Lee, “Generating datasets of 3d garments with sewing patterns,” *arXiv preprint arXiv:2109.05633*, 2021.
- [15] Maria Korosteleva and Sung-Hee Lee, “Neuraltailor: Reconstructing sewing pattern structures from 3d point clouds of garments,” *ACM Transactions on Graphics (TOG)*, vol. 41, no. 4, pp. 1–16, 2022.
- [16] Cheng-Hsiu Chen, Jheng-Wei Su, Min-Chun Hu, Chih-Yuan Yao, and Hung-Kuo Chu, “Panelformer: Sewing pattern reconstruction from 2d garment images,” in *Proceedings of the IEEE/CVF Winter Conference on Applications of Computer Vision*, 2024, pp. 454–463.
- [17] Chaitanya Patel, Zhouyingcheng Liao, and Gerard Pons-Moll, “Tailornet: Predicting clothing in 3d as a function of human pose, shape and garment style,” in *Proceedings of the IEEE/CVF conference on computer vision and pattern recognition*, 2020, pp. 7365–7375.
- [18] Boxiang Rong, Artur Grigorev, and et. al. Wang, “Gaussian garments: Reconstructing simulation-ready clothing with photorealistic appearance from multi-view video,” *arXiv preprint arXiv:2409.08189*, 2024.
- [19] Bernhard Kerbl, Georgios Kopanas, Thomas Leimkühler, and George Drettakis, “3d gaussian splatting for real-time radiance field rendering.,” *ACM Trans. Graph.*, vol. 42, no. 4, pp. 139–1, 2023.
- [20] Zorah Lahner, Daniel Cremers, and Tony Tung, “Deepwrinkles: Accurate and realistic clothing modeling,” in *Proceedings of the European conference on computer vision (ECCV)*, 2018, pp. 667–684.
- [21] Hongwen Zhang, Yating Tian, and et. al., “Pymaf: 3d human pose and shape regression with pyramidal mesh alignment feedback loop,” in *IEEE/CVF international conference on computer vision*, 2021.
- [22] Nanyang Wang, Yinda Zhang, Zhuwen Li, Yanwei Fu, Wei Liu, and Yu-Gang Jiang, “Pixel2mesh: Generating 3d mesh models from single rgb images,” in *European conference on computer vision (ECCV)*, 2018.
- [23] Naureen Mahmood, Nima Ghorbani, Nikolaus F Troje, Gerard Pons-Moll, and Michael J Black, “Amass: Archive of motion capture as surface shapes,” in *Proceedings of the IEEE/CVF international conference on computer vision*, 2019, pp. 5442–5451.
- [24] Olga Sorkine, “Laplacian mesh processing,” *Eurographics (State of the Art Reports)*, vol. 4, no. 4, pp. 1, 2005.
- [25] Olga Sorkine and Marc Alexa, “As-rigid-as-possible surface modeling,” in *Symposium on Geometry processing*. Citeseer, 2007, vol. 4, pp. 109–116.